Three-Dimensional Directionality Is a Pivotal Structural Feature for the Bioactivity of Azabisphosphonate-Capped Poly(PhosphorHydrazone) Nanodrug Dendrimers

Three-dimensional directionality is a pivotal structural feature for the bioactivity of azabisphosphonate-capped Poly(PhosphorHydrazone) nanodrug dendrimers.

Journal:	*Biomacromolecules*
Manuscript ID	bm-2017-013985
Manuscript Type:	Article
Date Submitted by the Author:	29-Sep-2017
Complete List of Authors:	Hayder, Myriam; Centre de Physiopathologie de Toulouse-Purpan Garzoni, Matteo; University for Applied Sciences of Southern Switzerland (SUPSI), Laboratory of Applied Mathematics and Physics (LaMFI) Bochicchio, Davide; University of Applied Sciences and Arts of Southern Switzerland (SUPSI), DTI Caminade, Anne-Marie; Laboratoire de Chimie de Coordination, Team of Dendrimers and Heterochemistry COUDERC, François; Université Paul Sabatier, Laboratoire IMRCP Ong-Meang, Varravaddheay; Universite Toulouse III Paul Sabatier, Laboratoire IMRCP Davignon, Jean-Luc; Centre de Physiopathologie de Toulouse-Purpan Turrin, Cédric-Olivier; CNRS, Laboratoire de Chimie de Coordination Pavan, Giovanni; University of Applied Science of Southern Switzerland, Department of Innovative Technologies Poupot, Remy; INSERM, U1043; CNRS, U5282; Université de Toulouse, UPS

Three-dimensional directionality is a pivotal structural feature for the bioactivity of azabisphosphonate-capped Poly(PhosphorHydrazone) nanodrug dendrimers.

Myriam Hayder,[†] Matteo Garzoni,[‡] Davide Bochicchio,[‡] Anne-Marie Caminade,[§] François Couderc,[‖] Varravaddheay Ong-Meang,[‖] Jean-Luc Davignon,[†] Cédric-Olivier Turrin,[*,§] Giovanni M. Pavan,[**,‡] and Rémy Poupot [***,†]

[†] *Centre de Physiopathologie de Toulouse-Purpan, Toulouse, F-31300, France; INSERM, U1043; CNRS, U5282; Université de Toulouse, UPS, France*

[‡] *Department of Innovative Technologies, University for Applied Sciences and Arts of Southern Switzerland (SUPSI), Galleria 2, Via Cantonale 2c, CH-6928 Manno, Switzerland*

[§] *Laboratoire de Chimie de Coordination, 205 route de Narbonne, BP 44099, Toulouse Cedex4, F-31077, France; CNRS, UPR8241; Université de Toulouse, UPS, INP, France*

[‖] *Laboratoire des IMRCP, 118 route de Narbonne, Toulouse Cedex9, F-31062, France; CNRS, U5623; Université de Toulouse, UPS, France*

* Corresponding author: Laboratoire de Chimie de Coordination, 205 route de Narbonne, BP44099, 31077 Toulouse Cedex4, France.

** Corresponding author: Department of Innovative Technologies, University for Applied Sciences and Arts of Southern Switzerland (SUPSI), Galleria 2, Via Cantonale 2c, CH-6928 Manno, Switzerland.

*** Corresponding author: INSERM 1043, CHU Purpan, BP3028, 31024 Toulouse Cedex3, France.

E-mail addressses: cedric-olivier.turrin@lcc-toulouse.fr (C.O. Turrin), giovanni.pavan@supsi.ch (G.M. Pavan), remy.poupot@inserm.fr (R. Poupot).

ABSTRACT

Dendrimers are nanosized, non-linear, hyperbranched polymers whose overall three-dimensional shape is key for their biological activity. Poly(PhosphorHydrazone) (PPH) dendrimers capped with aza-bisphosphonate (ABP) end groups are known to have anti-inflammatory properties enabling the control of inflammatory diseases in different mouse models. Here we screen the anti-inflammatory activity of a series of PPH bearing between 2 and 16 ABP end groups in a mouse model of arthritis, and confront the biological results with atomistic simulations of the dendrimers. We show that only the PPH dendrimers capped with 10 and 12 ABP end groups can control the flare of the inflammatory disease. All-atom accelerated molecular dynamics simulations show that dendrimers with low number of ABP end groups are directional but highly flexible/dynamic, and have thereby limited efficiency in establishing multivalent interactions. The largest dendrimer appears as non-directional, having 16 ABP end groups forming patches all over the dendrimer surface. Conversely, intermediate dendrimers having 10 or 12 ABP end groups reach the best compromise between the number of surface groups and their stable directional gathering, a real maximization of multivalency.

Keywords

Arthritis; Biodegradability; Dendrimers; Inflammation; Molecular dynamics

INTRODUCTION

Dendrimers are non-linear, hyperbranched nanomolecules whose potential biomedical applications generate a tremendous amount of attention and work. Dendrimers are built from a central core on which series of branches are added. At the end of each branch, a point of divergence enables the arborescent engraftment of the next series, leading to a "tree-like" molecule. The number of series of branches is called the generation of the dendrimer (e.g., a generation 1 dendrimer has one series of branches). Finally, the surface groups are added on the outermost series of branches. As polyvalent interactions are ubiquitous in biological systems,[1] the possibility to design molecules with controlled multivalency, such as dendrimers, is relevant for biomedical applications.[2] At least from this point of view, dendrimers are attractive molecules to biologists.[3,4] Poly(PhosphorHydrazone) (PPH) dendrimers ended with Aza-BisPhosphonate (ABP) groups have shown immuno-modulatory properties toward different populations of human immune cells.[5–8] In particular, the first generation PPH dendrimer capped with twelve ABP end groups (ABP dendrimer) displays anti-inflammatory properties, both *in vitro*[7,9,10] and *in vivo* in animal models of chronic[11,12] and acute[11,13] inflammatory contexts. This unique molecule is now considered a promising drug-candidate for the care of patients with chronic inflammatory diseases as it does not induce either general or immunological toxicity in non-human primates after repeated systemic injections.[14] In parallel to the assessment of the immuno-modulatory properties of the lead ABP dendrimer, we have explored the influence of different phosphonate-based surface groups,[5,6] of isosteric functions thereof,[15] and of size (i.e., generation)[6] of PPH dendrimers. We have also explored the influence of the local density of ABP surface functions of PPH dendrimers of the first generation towards the activation of human immune cells. In this way, we have shown that PPH dendrimers of the first generation displaying 8,

10, and 12 (the ABP dendrimer) promote the *in vitro* activation of human monocytes,[16] the proliferation of Natural Killer cells and somehow of circulating γδ T cells[8] which share functional features with both conventional αβ T cells and Natural Killer cells.[17] PPH dendrimers of the first generation having less than 8 (2, 4, and 6 have been tested) or more than 12 (16 has been tested) ABP terminal groups show a dramatic decrease or no activity at all. Recently, we have reported the first study assessing the influence of a large number of dendritic scaffolds (seven different families of dendrimers) ended by ABP terminal groups.[18] We have shown that the internal structure of dendrimers is not an inert or innocent support for active surface functions, but plays a crucial role, at least when considering biological properties. Indeed, the global three-dimensional shape of dendrimers with identical terminal groups, and the spatial distribution of these terminal groups depend on the nature of the scaffold. Regarding the anti-inflammatory activation of monocytes, the active dendrimers are those in which the surface functions are gathered on one side (directional molecules), likely the suitable orientation to display efficient multivalent interactions with target cells. In continuation of this pioneering study, here we have assessed the *in vivo* efficacy of a series of PPH dendrimers of the first generation having 2, 4, 8, 10, 12 (the ABP dendrimer), and 16 ABP terminal groups (Fig. 1). We used the mouse model of experimental arthritis induced by the transfer of K/BxN serum.[19] The bioactivities of the six dendrimers have been then confronted with the structural data obtained from all-atom Molecular Dynamics (MD) and accelerated MD (aMD) simulations thereof.

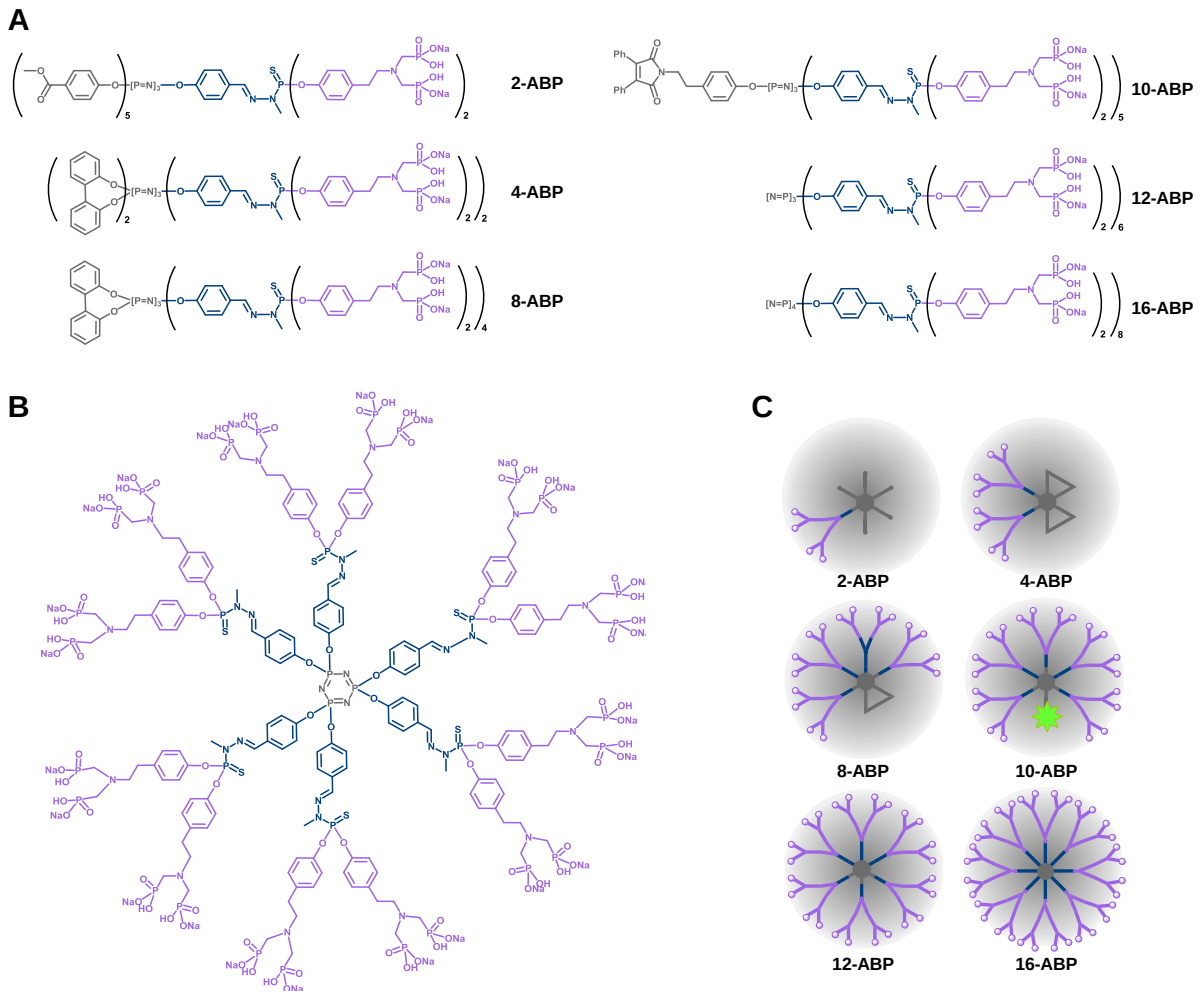

Figure 1. Structure of the ABP-capped PPH dendrimers used in this study. (A) Chemical structure of the complete series of dendrimers. (B) Two-dimensional structure of the dendrimer **12-ABP**. (C) Schematic representation of the complete library of dendrimers.

EXPERIMENTAL SECTION

Chemical syntheses. The six dendrimer compounds included in this study were synthesized as already described.[6,16]

The K/BxN serum transfer model of arthritis. 9-week old male BALB/cA mice were transferred at days 0 and 2 intraperitoneally with 200 µL of serum from 60-week old K/BxN mice. Following a prophylactic protocol, dendrimers were injected intravenously at days 1, 4, and 11. Mice were sacrificed 20 days after the first transfer of serum. The swelling of hind paws of K/BxN serum-transferred and control mice was measured using a calliper. In parallel, the severity of arthritis was assessed macroscopically in a blind fashion for each paw per mouse with a five-grade score (0, normal; 1, light swelling of the joint; 2, obvious swelling of the joint; 3, obvious swelling of the joint with redness of the footpad; 4, severe swelling; 5, severe swelling and immobile mouse).

All-atom simulations. The MD and aMD simulation work was performed using the AMBER 14 software.[20] The atomistic models for all ABP dendrimers were created and parametrized according to a validated procedure recently reported for the simulation of variants of these dendrimers,[18] and similar branched polymers in aqueous solution.[21–23] In particular, all dendrimers were parametrized according to the General Amber Force Field (GAFF).[24] In order to reproduce the biological experimental conditions, all dendrimer models were immerged in a periodic simulation box containing explicit TIP3P water molecules,[25] and a suitable number of counter-ions to guarantee the overall neutrality of the systems and to reproduce the ionic strength of 150 mM NaCl. After preliminary minimization, all molecular systems underwent 200 ns of classical MD in NPT (constant number of N: atoms, P: pressure, and T: temperature in the system) conditions at 37 °C of temperature and 1 atm of pressure. All simulations conducted in this study used a time step of 2 fs, a 10 Å cutoff, the SHAKE algorithm to constrain bonds involving hydrogens,[26] and the Particle Mesh Ewald (PME) to treat long-range electrostatics.[27]

During these preliminary MD runs, all dendrimers were seen to reach an equilibrium configuration in the MD regime with good stability. Several parameters such as the evolution of the radius of gyration (R_g), Solvent Accessible Surface Area (SASA), Root Mean square Displacement (RMD), and energy of the dendrimers were used to monitor the equilibration of the dendrimers in solution.

To improve the exploration of the conformational space of the six dendrimers (see below), we have used aMD as implemented in AMBER 14,[28] starting from the pre-equilibrated configurations for the dendrimers obtained from the MD. In the aMD runs (400 ns) we have applied the bias to both the whole potential energy and the dihedral term, where the bias parameters for the former (*AlphaP*) and for the latter (*AlphaD*) have been calculated using the standard approach used in previous aMD studies reported in literature.[28–32]

(1) $AlphaP = 0.16\left[\frac{kcal}{mol}\right] \times N_{atoms}$ (2) $AlphaD = \frac{1}{5} \times 4\left[\frac{kcal}{mol\ res}\right] \times N_{res}$.

The threshold values for the whole potential energy (*EthreshP*) and for the dihedral term (*EthreshD*) of the simulated systems have been set to:

(3) $EthreshP = Epot + AlphaP$ (4) $EthreshD = Edih + 5 \times AlphaD$,

where *Epot* and *Edih* are the reference equilibrated values taken from the preliminary classical MD simulation. The aMD trajectories have been further reweighted to obtain the Free Energy Surfaces (FES) of Fig. 4A according to the procedure reported elsewhere.[28]

RESULTS AND DISCUSSION

Efficacy of dendrimers to control arthritis in the mouse model of K/BxN serum transfer. The series of ABP-capped dendrimers involved in this study encompasses 6 compounds: **2-ABP**, **4-ABP**, **8-ABP**, **10-ABP**, **12-ABP** and **16-ABP**. The compound with six ABP end groups at its surface (potentially **6-ABP**), although synthesized, was not included as

it is not possible to design a synthetic strategy to obtain an isomolecular batch of this compound. Indeed, the locked position on the second phosphorus atom cannot be controlled and is statistical, leading to the synthesis of a mixture of two different **6-ABP** compounds differing by the relative positions of the PPH branches which bear the six ABP groups.[16] Dendrimer **10-ABP** is a fluorescent derivative in which one of the six branches was replaced by a fluorescent julolidine group, enabling the follow-up of the compound when interacting with biological material.[16] The anti-inflammatory properties of the six ABP-capped dendrimers have been assessed in the widely used mouse model of experimental arthritis induced by the transfer of K/BxN serum (also known as the KRN mouse model).[19] In this model, inflammation and arthritis are rapidly and transiently induced by transferring serum from autoimmune K/BxN mice into wild-type BALB/cA mice. This model relies on the presence of antibodies specific for the auto-antigen Glucose-6-Phosphate Isomerase, which develop in autoimmune K/BxN mice. The effect of dendrimers was tested by intravenous injection at the concentration of 10 mg/kg following a preventive protocol we have already described:[11] dendrimers were injected intravenously at day 1 – between the first and the second injection of the K/BxN serum – and then again at days 4 and 11. The daily measurement of the swelling of paws is indicative of the onset and the development of the inflammation of joints. Along the study, the dendrimers **10-ABP** and **12-ABP** have shown the ability to prevent the flare of inflammation induced by the K/BxN serum in the mice. Indeed, the size of the paws in these groups ended at the same level than in the control group of healthy mice (Fig. 2A). Based on the swelling of paws, the redness of the footpad, and the mobility of the animals, a clinical score was established on a daily basis (clinical arthritic score as the sum of individual scores for each paw; maximal score of 5 for one paw, i.e., 20 for an animal). There also, the same two dendrimers can control and reverse the development of the disease (Fig. 2B). Overall, based on the swelling of paws and the arthritic score, the

incidence of arthritis (i.e., the percentage of diseased animals) in each group is plotted in Fig. 2C. It clearly shows that only dendrimers **10-ABP** and **12-ABP** have a therapeutic effect on arthritis in this model.

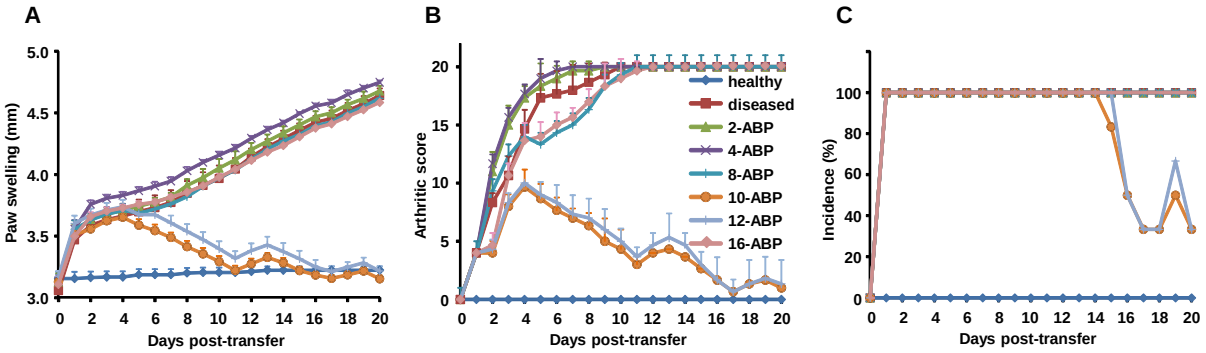

Figure 2. Efficacy of dendrimers to control arthritis in the mouse model of K/BxN serum transfer. (A) Measurement of the swelling of paws (n=6 mice for each condition), (B) evaluation of the arthritic score (n=6 mice for each condition), and (C) incidence of arthritis during the assay.

Regarding dendrimers **10-ABP** and **12-ABP**, the results obtained here are in concordance with the *in vitro* anti-inflammatory activation of human monocytes assessed formerly with this series of dendrimers.[16] Surprisingly, dendrimer **8-ABP** is not active in the mouse model of arthritis, whereas it was one of the most active regarding the *in vitro* activation of human monocytes.[16] To explain this discrepancy, we have studied the hydrolytic degradation of the **12-ABP** dendrimer in water solutions.

Biodegradability of the ABP-capped PPH dendrimers. Although the **12-ABP** dendrimer is stable as dry powder for months when stored at -20°C, aqueous solutions of this compound have been showed to slowly degrade according to a mechanism that has been partially identified. Under smooth conditions, at physiological pH and 37°C, aqueous solutions of **12-ABP** undergo a slow degradation which is traduced by the appearance on ^{31}P

NMR spectra of a singlet at 66.25 ppm (Fig. 3A). The appearance of this new singlet at 66.25 ppm is accompanied by the appearance of a side peak at the foot of the singlet centred on 63.75 ppm, accounting for P=S phosphorus atoms of the divergent point and traducing the dissymetrization of the molecule.

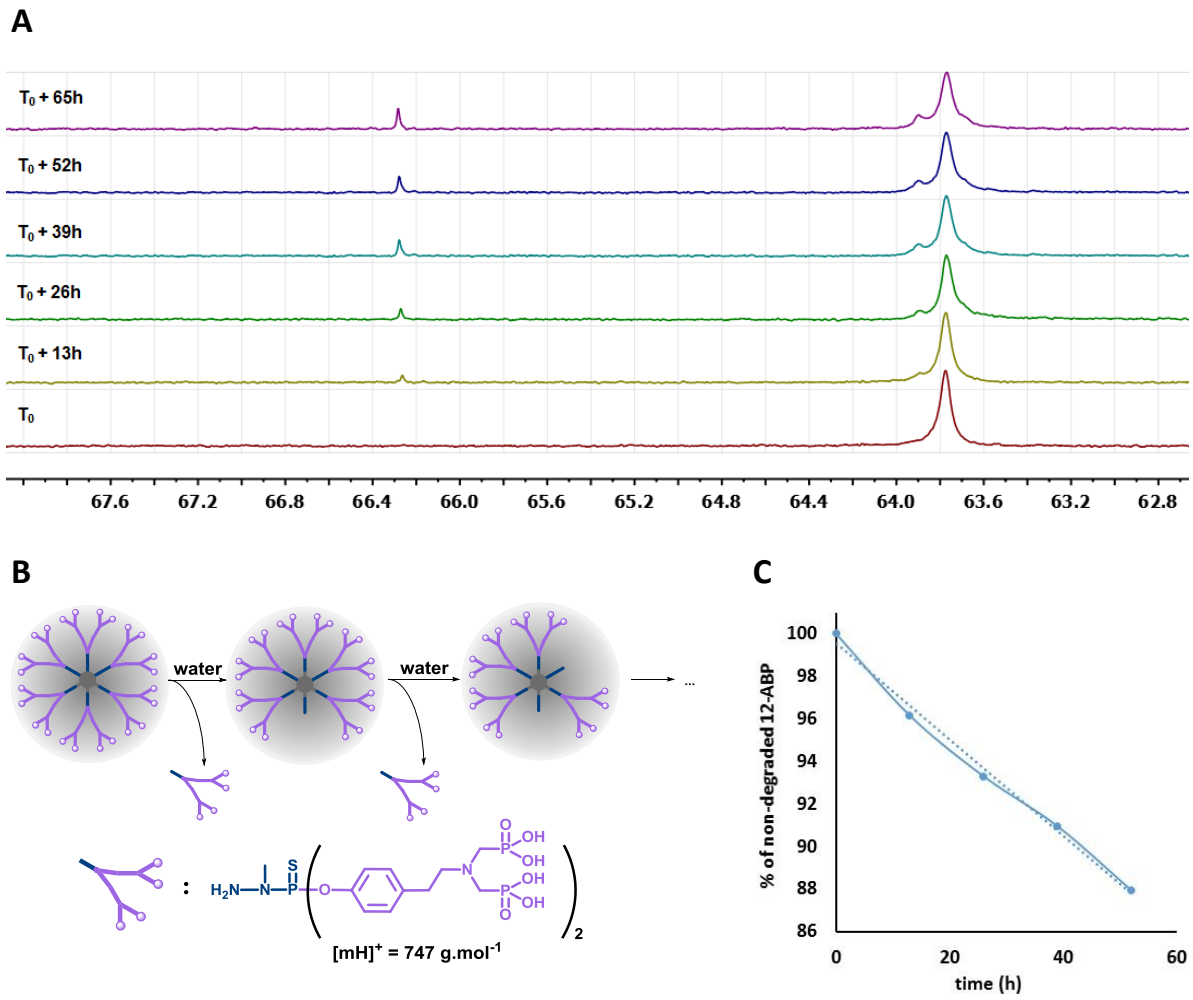

Figure 3. Biodegradability of the 12-ABP dendrimer. (A) Spontaneous hydrolysis of the **12-ABP** dendrimer in water solution (pH = 7.2, 37°C) monitored by ^{31}P NMR. (B) Spontaneous hydrolysis of the **12-ABP** dendrimer involves the breaking of hydrazone bounds. (C) Hydrolysis of the **12-ABP** dendrimer follows a zero order kinetics.

We have already shown in previous studies that the hydrazone linkage (CH=N-N) of PPH dendrimers is the weak point of these macromolecules regarding their stability. For instance,

we have demonstrated quite early that these linkages undergo a clear hydrolytic-like degradation during Electrospray Ionisation or MALDI TOF Mass Spectrometry experiments.[33] In this respect, it should be pointed out that similar mechanisms involving the progressive loss of branches have already been identified during mass spectrometry experiments on the **12-ABP** dendrimer, as revealed by the presence of successive isotopic patterns of the various sodium forms separated by an m/z of 757 $g.mol^{-1}$ accounting for the protonated form of a side product resulting from the breaking of the hydrazone bound (Figure S1). In addition to this bundle of data accounting for the breaking of CH=N hydrazone weak point, the NMR monitoring also included ^{1}H-NMR and 2D correlation experiments which showed on ^{1}H spectra the progressive decrease of the signal accounting for the CH=N centred on 8 ppm and the appearance of new signals in the aromatic region (Figure S2) that were found to correlate with the tyramine moiety bearing the aminobisphosphonate tweezer (FigureS3 and Figure S4). Additionally, DOSY experiments confirmed that these signals belong to a molecular entity with a diffusion coefficient significantly lower than the one observed for the non-degraded **12-ABP** dendrimer (data not shown). Consequently, the hydrolytic degradation of the **12-ABP** dendrimer in water solution at pH = 7.2 and at 37°C, that is somehow close to some of the key physiological parameters, involves the breaking of hydrazine bounds, and the progressive release of a trifunctional thiophosphorus atom (Fig. 3B) having an unambiguous signature on ^{31}P NMR spectra at 66.25 ppm, a chemical shift which is actually in agreement with previous studies on comparable structures.[34] Despite the preliminary aspect of this hydrolytic degradation study, the ratio of the integrate value of the CH=N singlet divided by the sum of the integrate values of aromatic signals showed a progressive degradation process that follows a zero order kinetics (Fig. 3C).

The hydrazone linkage (CH=N-N) is found in branches of all the PPH dendrimers. This means that the 6 dendrimers of the series used in this study undergo hydrolysis in aqueous

solution, although the kinetics may be dependent on the dendrimer. The biodegradability of PPH dendrimers could explain why the **8-ABP** dendrimer has been found bio-active in short-term *in vitro* experiments,[16] whereas it is not active in longer experiments *in vivo* (this study). Indeed, as soon as it has lost one branch, the **8-ABP** dendrimer is no more active, whereas the **10-ABP** and the **12-ABP** dendrimers have to loose several branches before losing their activity, thereby having a prolonged action.

All-atom molecular dynamics simulations of the dendrimers in explicit solvent. Molecular modelling was used to try to understand the molecular origin for the striking differences observed in the *in vivo* biological properties. In order to gain molecular-level information on the dendrimers in the biological environment, all-atom MD simulations of the six dendrimers in solution were carried out at 37°C in the presence of explicit water molecules and NaCl (150 mM). Each molecular system has been preliminary equilibrated during 200 ns of MD simulation as described previously.[18,35] Different data, such as, for example, the R_g of dendrimers have been extracted from the MD trajectories (Fig. 4A: solid and dotted black lines represent R_g and SASA average values and standard deviations, respectively).

Recently, it has been demonstrated by using advanced sampling methods that the intrinsic sampling limitations of classical MD can limit the exploration of the dendrimer structure in the solvent, especially for semi-flexible structures.[21,36] For this reason, here we have used aMD,[29] an advanced sampling technique recently proven useful for the exploration of the conformational space of semi-flexible macromolecules (e.g., proteins, peptides, etc...) in aqueous solution.[30,31] For example, it has been recently shown that the conformational exploration of a complex macromolecule (e.g., a protein) in solution provided by aMD in

hundreds of nanoseconds is comparable to that obtainable with classical MD in the timescale of milliseconds.[32]

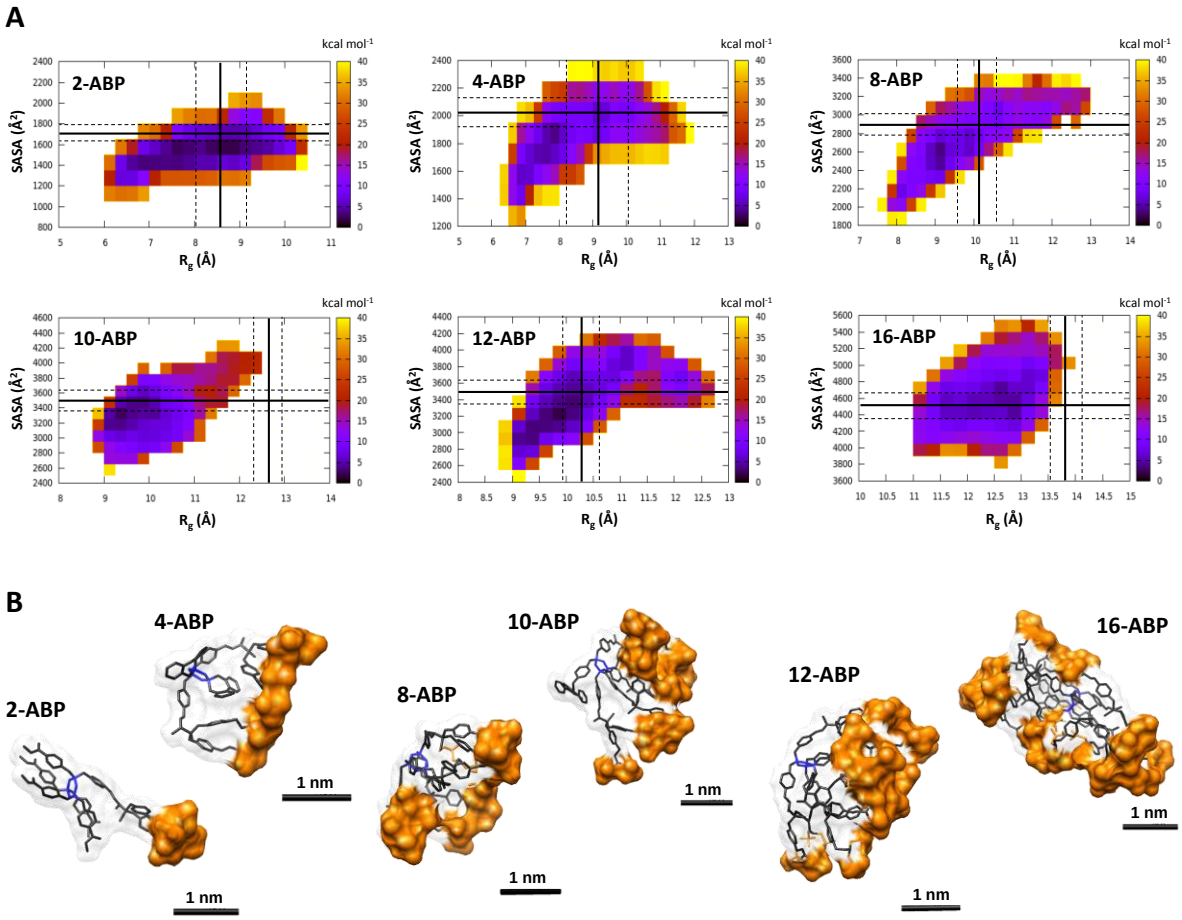

Figure 4. All-atom aMD simulations of the dendrimers in explicit solvent. (A) FES of the dendrimers from the aMD simulations represented as a function of the R_g and SASA of the dendrimer. Solid black lines represent the R_g and SASA average values obtained from the preliminary MD simulations (dotted lines: standard deviations); dark colors in the FES identify the most energetically favored configurations for the dendrimers in solution. (B) Equilibrium conformations for the six dendrimers, corresponding to the minima of the FES (violet). The phosphonate groups of the dendrimers are represented in orange, the scaffold in black, and the core of the dendrimers in blue.

Starting from the equilibrium conformations for the dendrimers obtained from our preliminary MD – solid black lines in Fig. 4A identify the latter in terms of R_g and SASA of the dendrimers –, all systems underwent 400 ns of aMD in the same conditions. During the aMD simulations, the dendrimers exhaustively explored their conformational space. Reweighting of the aMD trajectories allowed to estimate the FES of the different dendrimers in the solvent. Shown in Fig. 4A as a function of the R_g and SASA of the dendrimers, the darkest regions in the FES identify minimum energy (most favorable) conformations. On average, the dendrimers can better fold (reduced R_g and SASA) during the aMD compared to the MD simulations. This is consistent to what recently seen by using a different advanced sampling approach (well-tempered metadynamics) on PEGylated dendrimer analogues.[21,36] Fig. 4B shows the equilibrium conformations for the six dendrimers in the solvent, corresponding to the minima of the FES (violet). Consistent with what recently seen for similar dendrimers,[18] it is clear that in all dendrimers the aza-bisphosphonate surface groups of the dendrimers tend to clusterize due to the interaction with oppositely charged ions from dissolved NaCl present in solution. Visually, all dendrimers assume a directional conformation, with the active groups gathered on one side, with the exception of dendrimer **16-ABP**. In this case, clusters of aza-bisphosphonate units are spread all over the surface of the dendrimer (Fig. 4B).

We performed a statistical analysis of the aMD trajectories to quantify the clustering/compartmentalization and the relative dynamics of the surface groups around the dendrimers. These are factors determining the overall directionality of the dendrimer, directly related to the ability of the latter to establish multivalent interactions with its bio-targets.[18] To this end we monitored the displacement of the aza-bisphosphonate units during the aMD runs on the three *x*, *y* and *z* directions. This allowed us to subdivide the six dendrimers into three main categories – (i) those dendrimers intrinsically directional (possessing just one or two

branches, i.e., dendrimers **2-ABP** and **4-ABP**), but having limited possibility of establishing multivalent interactions, (ii) directional dendrimers, where multiple surface groups are stably clusterized on the surface (dendrimers **8-ABP**, **10-ABP**, and **12-ABP**), and (iii) non directional dendrimers, where clusters of surface groups are present all around the surface (dendrimer **16-ABP**). On one hand in (i), the aza-bisphosphonate units are intrinsically displayed in directional way, but the limited surface crowding produces dynamic oscillation/vibration of the end groups. On the other hand, in (ii) and (iii) the folded conformation of the dendrimer is more stable, and the dendrimers can be represented as globular objects with (more or less) static aza-bisphosphonate patches on the surface – the latter resulting in a directional (ii) or non-directional (iii) displacement of active units.

Using the centres of the dendrimers (red squares) as a reference, we calculated from the aMD trajectories the average position of the aza-bisphosphonate units (black crosses) during the runs on the three planes *xy*, *xz*, *yz*, obtaining the "planar directionality vectors" δ_{xy}, δ_{xz} and δ_{yz} reported in Fig. 5A. The vectorial sum of δ_{xy}, δ_{xz} and δ_{yz} provided us with the directionality vector δ, indicative of the overall anisotropic distribution of the surface groups around the dendrimer core on the dendrimer surface. Dendrimers where the displacement of surface groups is rather uniform all around the surface, either in terms of static displacement (uniform surface crowding) or of dynamic fluctuating groups (statistically present/delocalized everywhere on the surface), will have δ tending to 0. Conversely, dendrimers with a persistent directional character will have increased δ value. In order to compare between different sizes of the dendrimers, the δ vector has been further divided by the size of each dendrimer (R_g), obtaining the non-dimensional directionality score (*d*). This quantification enables the subdivision of the series of dendrimer into three groups, as shown in Fig. 5B.

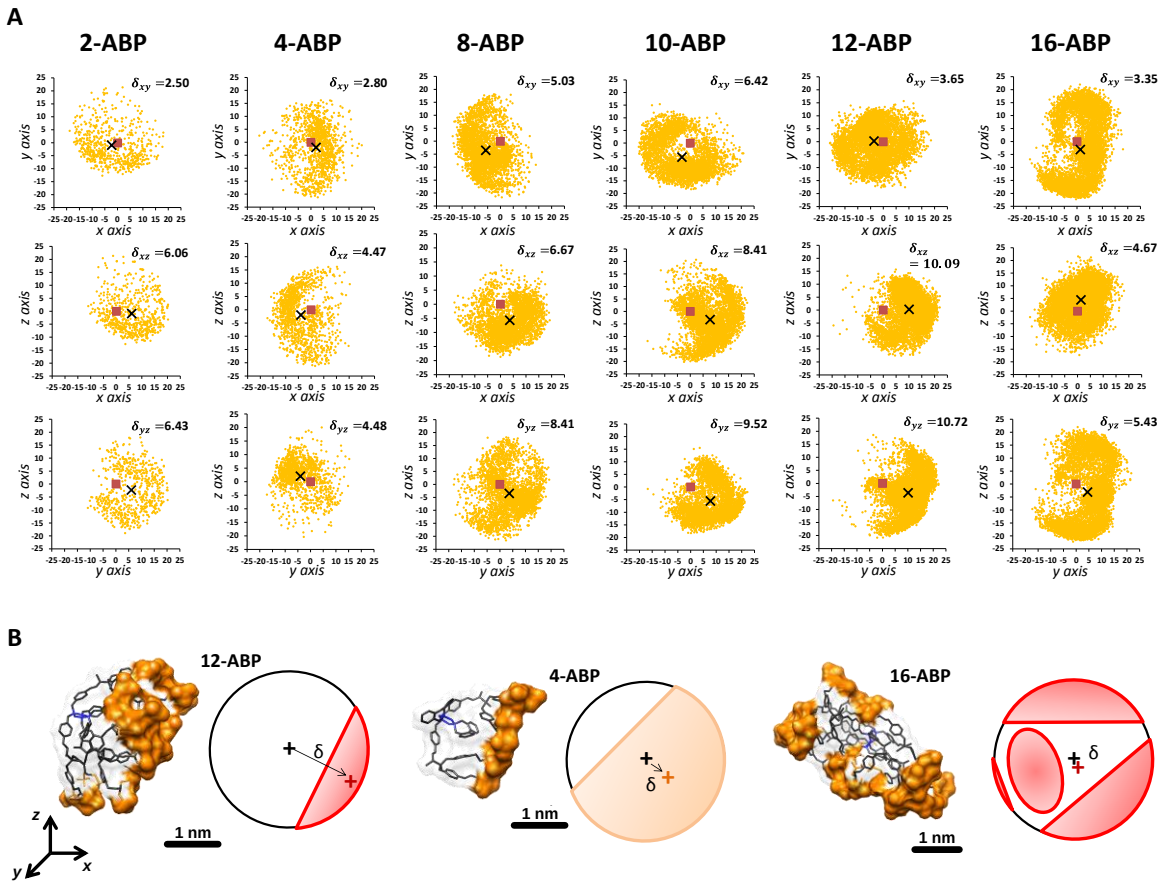

Figure 5. Characterization of the directionality of the dendrimers. (A) Displacement of the aza-bisphosphonate groups (black cross) respect to the centres of the dendrimers (red square), and calculated values of the relative δ_{xy}, δ_{xz} and δ_{yz} vectors. (B) The dendrimers can be subdivided into stably directional multivalent dendrimers (e.g., **12-ABP**), dynamic dendrimers with low multivalency (e.g., **4-ABP**) and non-directional dendrimers (e.g., **16-ABP**).

This analysis allowed us to understand how much, and how stably, the surface groups are gathered together on the surface, providing a relative quantification of the effective directionality of the dendrimers (*d*) (Table 1).

	2-ABP	4-ABP	8-ABP	10-ABP	12-ABP	16-ABP
MW (Da)	1838.13	2397.33	4109.13	5258.89	5819.92	7759.90
δ (Å)	9.2	6.9	10.8	14.2	15.2	7.9
R_g[a] (Å)	8.5	7.8	9	9.5	10	12.7
d[b]	1.08	0.88	1.19	1.49	1.52	0.62

[a] R_g corresponding to the minimum energy conformations for the dendrimers (violet regions in the FES of Fig. 4A). [b] The non-dimensional directionality index d was calculated as: $d = \delta/R_g$.

It is clear how, for example, in intrinsically directional dendrimers **2-ABP** and **4-ABP**, the surface groups can freely move around the centres of the dendrimers. These dendrimers have low surface crowding and limited possibility to establish stable multivalent interactions, due to lack of aza-bisphosphonate groups. This produces a relatively low directionality index $d \sim 1$. This is also somehow true for dendrimer **8-ABP**. Conversely, dendrimer **16-ABP** has a more rigid surface, and the aza-bisphosphonate groups are present all around the centre of the dendrimer. In this way the δ vector turns out to be small, and the directionality index d is the lowest among all dendrimers (~ 0.6). On the other hand, dendrimers **10-ABP** and **12-ABP** have larger δ vector, and directionality index reaching $d \sim 1.5$. Looking at Fig. 5B the distribution of the aza-bisphosphonate groups on the surface of these dendrimers is reminiscent of and umbrella (see for example plane *yz* for dendrimer **12-ABP**).

CONCLUSIONS

The experimental and theoretical studies reported in this paper provide new insights in the relationship between the overall conformation of ABP-capped PPH dendrimers in aqueous solution and their anti-inflammatory properties in an *in vivo* model of experimental arthritis. We observe striking differences in the conformation and dynamics that the PPH dendrimers

of the tested series assume in the solvent. These differences fit well with the observed anti-inflammatory trends. Indeed, the maximum value obtained for the *d* index demonstrates that dendrimers **10-ABP** and **12-ABP** reach the best compromise between the number of surface groups and their directional displacement on the surface, i.e., a real maximization of multivalency related to a specific bio-property of the dendrimers. Remarkably, the good agreement between the stable directionality of dendrimers, as analyzed from the atomistic simulations, and the bioactivity of the various dendrimers offers a useful parameter to draw structure-property relationships. Moreover, we have shown recently that PPH dendrimers mediate their anti-inflammatory activity through a specific recognition and binding with receptor(s) at the surface of human monocytes.[35] The further identification of these receptors will also help to understand how to customize the molecular structure of PPH dendrimers to control their specific bio-property.

ACKNOWNLEDGEMENT

M.G., D.B., and G.M.P. acknowledge the support from the Swiss National Science Foundation (SNSF grant: 2021_162827 to G.M.P.).

R.P. and C.O.T. acknowledge the institutional support of INSERM, CNRS, and the University of Toulouse. They also acknowledge the support from the “Agence Nationale de la Recherche” (ANR) and the “Direction Générale de l’Offre de Soins” (DGOS), project “TREE-DRUG” financed on the “Programme de Recherche Translationnelle en Santé 2013” (N° ANR-13-PRTS-0020).

ASSOCIATED CONTENT

Supplementary Material related to this article can be found at htpp://…

Supplementary Figure S1. Typical mass spectrum of **12-ABP** obtained by electrospray ionization. Supplementary Figure S2. ^{1}H NMR monitoring of the spontaneous hydrolysis of **12-ABP**. Supplementary Figure S3. HSQC [$^{1}H/^{13}C$-^{31}P(BB)] at T = 0 hr (upper spectrum) and T = 39 hr (lower spectrum). Supplementary Figure S4. HMBC [$^{1}H/^{13}C$-^{31}P(BB)] at T = 0 hr (upper spectrum) and T = 39 hr (lower spectrum).

REFERENCES

(1) Mammen, M.; Choi, S. K.; Whitesides, G. M. Polyvalent interactions in biological systems: implications for design and use of multivalent ligands and inhibitors. *Angew. Chem. Int. Ed.* **1998**, *37*, 2754–94.

(2) Varner, C. T.; Rosen, T.; Martin, J. T.; Kane, R. S. Recent advances in engineering polyvalent biological interactions. *Biomacromolecules* **2015**, *16*, 43–55.

(3) Hayder, M.; Fruchon, S.; Fournié, J. J.; Poupot, M.; Poupot, R. Anti-inflammatory properties of dendrimers per se. *Sci.World J.* **2011**, *11*, 1367–82.

(4) Fruchon, S.; Poupot, R. Pro-inflammatory versus anti-inflammatory effects of dendrimers: the two faces of immuno-modulatory nanoparticles. *Nanomaterials* **2017**, *7*, 251. doi:10.3390/nano7090251.

(5) Poupot, M.; Griffe, L.; Marchand, P.; Maraval, A.; Rolland, O.; Martinet, L.; L'Faqihi-Olive, F. E.; Turrin, C. O.; Caminade, A. M.; Fournié, J. J.; Majoral, J. P.; Poupot, R. Design of phosphorylated dendritic architectures to promote human monocyte activation. *FASEB J.* **2006**, *20*, 2339–51.

(6) Griffe, L.; Poupot, M.; Marchand, P.; Maraval, A.; Turrin, C. O.; Rolland, O.; Métivier, P.; Bacquet, G.; Fournié, J. J.; Caminade, A. M.; Poupot, R.; Majoral, J. P. Multiplication of human natural killer cells by nanosized phosphonate-capped dendrimers. *Angew. Chem. Int. Ed.* **2007**, *46*, 2523–26.

(7) Portevin, D.; Poupot, M.; Rolland, O.; Turrin, C. O.; Fournié, J. J.; Majoral, J. P.; Caminade, A. M.; Poupot, R. Regulatory activity of azabisphosphonate-capped dendrimers on human $CD4^+$ T cell proliferation for ex-vivo expansion of NK cells from PBMCs and immunotherapy. *J. Transl. Med.* **2009**, *7*, 82. doi: 10.1186/1479-5876-7-82.

(8) Poupot, M.; Turrin, C. O.; Caminade, A. M.; Fournié, J. J.; Attal, M.; Poupot, R.; Fruchon, S. Poly(phosphorhydrazone) dendrimers: yin and yang of monocyte activation for human NK cell amplification applied to immunotherapy against Multiple Myeloma. *Nanomedicine* **2016**, *12*, 2321–30.

(9) Fruchon, S.; Poupot, M.; Martinet, L.; Turrin, C. O.; Majoral, J. P.; Fournié, J. J.; Caminade, A. M.; Poupot, R. Anti-inflammatory and immuno-suppressive activation of human monocytes by a bio-active dendrimer. *J. Leukoc. Biol.* **2009**, *85*, 553–62.

(10) Degboé, Y.; Fruchon, S.; Baron, M.; Nigon, D.; Turrin, C. O.; Caminade, A. M.; Poupot, R.; Cantagrel, A.; Davignon, J. L. Modulation of pro-inflammatory activation of monocytes and dendritic cells by aza-bis-phosphonate dendrimer as an experimental therapeutic agent. *Arthritis Res. Ther.* **2014**, *16*, R98.

(11) Hayder, M.; Poupot, M.; Baron, M.; Nigon, D.; Turrin, C. O.; Caminade, A. M.; Majoral, J. P.; Eisenberg, R. A.; Fournié, J. J.; Cantagrel, A.; Poupot, R.; Davignon, J. L. Phosphorus-based dendrimer as nanotherapeutics targeting both inflammation and osteoclastogenesis in experimental arthritis. *Sci. Transl. Med.* **2011**, *3*, 81ra35. doi: 10.1126/scitranslmed.3002212.

(12) Hayder, M.; Varilh, V.; Turrin, C. O.; Saoudi, A.; Caminade, A. M.; Poupot, R.; Liblau, R. S. Phosphorus-based dendrimer ABP treats neuroinflammation by promoting IL-10-producing CD4+ T cells. *Biomacromolecules* **2015**, *16*, 3425–33.

(13) Fruchon, S.; Caminade, A. M.; Abadie, C.; Davignon, J. L.; Combette, J. M.; Turrin, C. O.; Poupot, R. An azabisphosphonate-capped poly(phosphorhydrazone) dendrimer for the treatment of endotoxin-induced uveitis. *Molecules* **2013**, *18*, 9305–16.

(14) Fruchon, S.; Mouriot, S.; Thiollier, T.; Grandin, C.; Caminade, A. M.; Turrin, C. O.; Contamin, H.; Poupot, R. Repeated intravenous injections in non-human primates demonstrate preclinical safety of an anti-inflammatory phosphorus-based dendrimer. *Nanotoxicology* **2015**, *9*, 433–41.

(15) Rolland, O.; Turrin, C. O.; Bacquet, G.; Poupot, R.; Poupot, M.; Caminade, A. M.; Majoral, J. P. Efficient synthesis of phosphorus-containing dendrimers capped with isosteric functions of amino-bis(methylene) phosphonic acids. *Tetrahedron Lett.* **2009**, *50*, 2078–82.

(16) Rolland, O.; Griffe, L.; Poupot, M.; Maraval, A.; Ouali, A.; Coppel, Y.; Fournié, J. J.; Bacquet, G.; Turrin, C. O.; Caminade, A. M.; Majoral, J. P.; Poupot, R. Tailored control and optimisation of the number of phosphonic acid termini on phosphorus-containing dendrimers for the ex-vivo activation of human monocytes. *Chem. Eur. J.* **2008**, *14*, 4836–50.

(17) Pont, F.; Familiades, J.; Déjean, S.; Fruchon, S.; Cendron, D.; Poupot, M.; Poupot, R.; L'Faqihi-Olive, F.; Prade, N.; Ycart, B.; Fournié, J. J. The gene expression profile of phosphoantigen-specific human γδ T lymphocytes is a blend of αβ T cell and NK cell signatures. *Eur. J. Immunol.* **2012**, *42*, 228–40.

(18) Caminade, A. M.; Fruchon, S.; Turrin, C. O.; Poupot, M.; Ouali, A.; Maraval, A.; Garzoni, M.; Maly, M.; Furer, V.; Kovalenko, V.; Majoral, J. P.; Pavan, G. M.; Poupot, R. The key role of the scaffold on the efficiency of dendrimer nanodrugs. *Nat. Commun.* **2015**, *6*, 7722. doi: 10.1038/ncomms8722.

(19) Kyburz, D.; Corr, M. The KRN mouse model of inflammatory arthritis. *Springer Semin. Immunopathol.* **2003**, *25*, 79–90.

(20) Case, D. A.; Babin, V.; Berryman, J. T.; Betz, R. M.; Cai, Q.; Cerutti, D. S.; Cheatham, T. E. III; Darden, T. A.; Duke, R. E.; Gohlke, H.; Goetz, A. W.; Gusarov, S.; Homeyer, N.; Janowski, P.; Kaus, J.; Kolossváry, I.; Kovalenko, A.; Lee, T. S.; LeGrand, S.; Luchko, T.; Luo, R.; Madej, B.; Merz, K. M.; Paesani, F.; Roe, D. R.; Roitberg, A.; Sagui, C.; Salomon-Ferrer, R.; Seabra, G.; Simmerling, C. L.; Smith, W.; Swails, J.; Walker, R. C.; Wang, J.; Wolf, R. M.; Wu, X.; Kollman, P. A. AMBER 14, **2014**, University of California, San Francisco.

(21) Pavan, G. M.; Barducci, A.; Albertazzi, L.; Parrinello, M. Combining metadynamics simulation and experiments to characterize dendrimers in solution. *Soft Matter* **2013**, *9*, 2593–7.

(22) Garzoni, M.; Okuro, K.; Ishii, N.; Aida, T.; Pavan, G. M. Structure and shape effects of molecular glue on supramolecular tubulin assemblies. *ACS Nano* **2014**, *8*, 904–14.

(23) Simanek, E. E.; Enciso, A. E.; Pavan, G. M. Computational design principles for the discovery of bioactive dendrimers: [s]-triazines and other examples. *Exp. Opin. Drug Disc.* **2013**, *8*, 1057–69.

(24) Wang, J.; Wolf, R. M.; Caldwell, J. W.; Kollman, P. A.; Case, D. A. Development and testing of a general amber force field. *J. Comput. Chem.* **2004**, *25*, 1157–74.

(25) Jorgensen, W. L.; Chandrasekhar, J.; Madura, J. D.; Impey, R. W.; Klein, M. L. Comparison of simple potential functions for simulating liquid water. *J. Chem. Phys.* **1983**, *79*, 926–35.

(26) Kräutler, V.; van Gunsteren, W. F.; Hünenberger, P. H. A fast SHAKE algorithm to solve distance constraint equations for small molecules in molecular dynamics simulations. *J. Comput. Chem.* **2001**, *22*, 501–8.

(27) Darden, T.; York, D.; Pedersen, L. Particle mesh Ewald: an N-log(N) method for Ewald sums in large systems. *J. Chem. Phys.* **1993**, *98*, 10089–92.

(28) Pierce, L. C. T.; Salomon-Ferrer, R.; de Oliveira, C. A. F.; McCammon, J. A.; Walker, R. C. Routine access to millisecond time scale events with accelerated molecular dynamics. *J. Chem. Theory Comput.* **2012**, *8*, 2997–3002.

(29) Hamelberg, D.; Mongan, J.; McCammon, J. A. Accelerated molecular dynamics: a promising and efficient simulation method for biomolecules. *J. Chem. Phys.* **2004**, *120* 11919–29.

(30) Miao, Y.; Feixas, F.; Eun, C.; McCammon, J. A. Accelerated molecular dynamics simulations of protein folding. *J. Comput. Chem.* **2015**, *36*, 1536–49.

(31) Bucher, D.; Grant, B. J.; Markwick, P. R.; McCammon, J. A. Accessing a hidden conformation of the maltose binding protein using accelerated molecular dynamics. *PLoS Comput. Biol.* **2011**, *7*, e1002034. doi: 10.1371/journal.pcbi.1002034.

(32) de Oliveira, C. A. F.; Grant, B. J.; Zhou, M.; McCammon, J. A. Large-scale conformational changes of Trypanosoma cruzi proline racemase predicted by accelerated molecular dynamics simulation. *PLoS Comput. Biol.* **2011**, *7*, e1002178. doi: 10.1371/journal.pcbi.1002178.

(33) Blais, J. C.; Turrin, C. O.; Caminade, A. M.; Majoral, J. P. MALDI TOF mass spectrometry for the characterization of phosphorus-containing dendrimers. Scope and limitations. *Anal. Chem.* **2001**, *72*, 5097–105.

(34) Colombo, D.; Caminade, A. M.; Majoral, J. P. Functionalized macrocycles incorporating phosphorus-nitrogen and phosphorus-oxygen bonds. Strategies of synthesis. *Inorg. Chem.* **1991**, *18*, 3365–7.

(35) Ledall, J.; Fruchon, S.; Garzoni, M.; Pavan, G. M.; Caminade, A. M.; Turrin, C. O.; Blanzat, M.; Poupot, R. Interaction studies reveal specific recognition of an anti-inflammatory polyphosphorhydrazone dendrimer by human monocytes. *Nanoscale* **2015**, *7*, 17672–84.

(36) Hameau, A.; Fruchon, S.; Bijani, C.; Barducci, A.; Blanzat, M.; Poupot, R.; Pavan, G. M.; Caminade, A. M.; Turrin, C. O. Theoretical and experimental characterization of amino-PEG-phosphonate-terminated PolyPhosphorHydrazone dendrimers. Influence of size and PEG capping on cytotoxicity profiles. *J. Polym. Sci. Polym. Chem.* **2015**, *53*, 761–74.

Graphical Abstract to:

Three-dimensional directionality is a pivotal structural feature for the bioactivity of azabisphosphonate-capped Poly(PhosphorHydrazone) nanodrug dendrimers.

Myriam Hayder,[†] Matteo Garzoni,[‡] Davide Bochicchio,[‡] Anne-Marie Caminade,[§] François Couderc,[‖] Varravaddheay Ong-Meang,[‖] Jean-Luc Davignon,[†] Cédric-Olivier Turrin,[*,§] Giovanni M. Pavan,[**,‡] and Rémy Poupot [***,†]

[†] *Centre de Physiopathologie de Toulouse-Purpan, Toulouse, F-31300, France; INSERM, U1043; CNRS, U5282; Université de Toulouse, UPS, France*

[‡] *Department of Innovative Technologies, University for Applied Sciences and Arts of Southern Switzerland (SUPSI), Galleria 2, Via Cantonale 2c, CH-6928 Manno, Switzerland*

[§] *Laboratoire de Chimie de Coordination, 205 route de Narbonne, BP 44099, Toulouse Cedex4, F-31077, France; CNRS, UPR8241; Université de Toulouse, UPS, INP, France*

[‖] *Laboratoire des IMRCP, 118 route de Narbonne, Toulouse Cedex9, F-31062, France; CNRS, U5623; Université de Toulouse, UPS, France*

* Corresponding author: Laboratoire de Chimie de Coordination, 205 route de Narbonne, BP44099, 31077 Toulouse Cedex4, France.

** Corresponding author: Department of Innovative Technologies, University for Applied Sciences and Arts of Southern Switzerland (SUPSI), Galleria 2, Via Cantonale 2c, CH-6928 Manno, Switzerland.

*** Corresponding author: INSERM 1043, CHU Purpan, BP3028, 31024 Toulouse Cedex3, France.

E-mail addressses: cedric-olivier.turrin@lcc-toulouse.fr (C.O. Turrin), giovanni.pavan@supsi.ch (G.M. Pavan), remy.poupot@inserm.fr (R. Poupot).

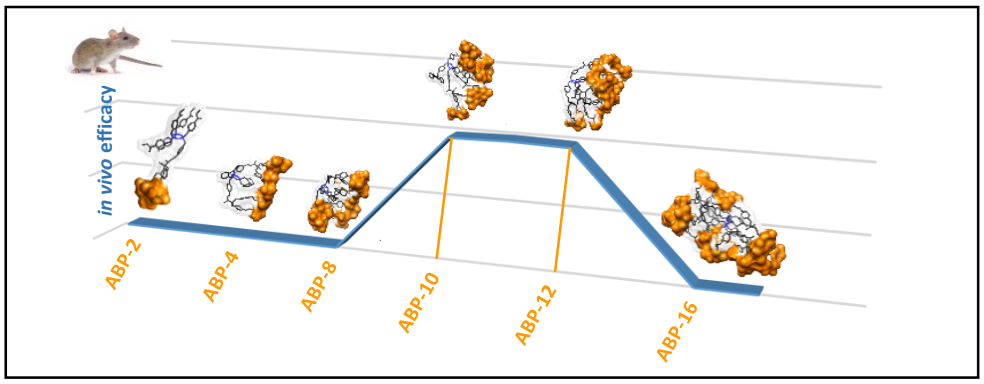
in vivo efficacy
ABP-2
ABP-4
ABP-8
ABP-10
ABP-12
ABP-16